ELSEVIER

# Enhancement of heat exchanger performance using combined electrohydrodynamic and passive methods

**R. S. Neve and Y. Y. Yan**
Thermo-Fluids Engineering Research Centre, Department of Mechanical Engineering and Aeronautics, City University, London, UK

Improvements are shown in the performance of heat exchangers fitted with passive enhanced tube surfaces by applying up to 30 kV between those surfaces and a surrounding electrode. In this context, enhancement means the addition of corrugations or more complicated surface irregularities, leading to increased surface area and modified bubble contact angles. Although it is now banned, R114 was used as the working fluid, so comparison could be made with previous published work. Equations are derived showing that a local electric field gradient will enhance nucleation rate and decrease critical bubble radius, both leading to improved heat transfer rate. Computational analysis has been used to show that the shapes of passive enhanced surfaces potentially create considerable increases in local field gradient to produce such favourable conditions. An additional by-product is that at far-field strengths of above some 1 kV/mm, boiling hysteresis seems to be eliminated.

**Keywords:** heat exchangers; electrohydrodynamic (EHD); enhancement; passive

## Introduction

In the next century, such renewable energy sources as solar, geothermal, and ocean thermal energy conversion (OTEC) will need to make a major impact in the sense of conserving current energy stocks and in terms of assisting environmental protection. This would be more practicable if the efficiency of conventional heat exchangers could be improved, especially those dealing with evaporation at low superheat conditions ($\Delta T < 10$ K) and with low quality waste heat recovery ($T < 100$°C). Improvements in heat transfer rates have been effected by using such passive methods as corrugated surfaces and surface tension devices and such active ones as mechanical vibration, injection, suction, and electric fields. Bergles (1985) has reviewed much of the literature on passive devices and reports that noticeably higher heat transfer rates can be achieved, but there is only minimal effect on boiling hysteresis. Bergles (1989), in a later paper, and Webb and Pais (1992) have reported test results on surfaces of the Gewa-T$^{TM}$ type. Clearly, improvements result from the greater probability of active sites for bubble formation over the increased surface areas. Although the possibility of heat transfer enhancement using applied electric fields has been known for many years (Choi 1961, 1962) more widespread investigation dates from the 1970s, this work having been reviewed by Jones (1978). More recently, Allen and Cooper (1987); Karayiannis et al. (1989); Cooper (1990); Ohadi et al. (1992); Ogata and Yabe (1993), and Barletta and Zanchini (1993) have all reported marked improvements in performance and the probable elimination of boiling hysteresis when electric field gradients of around 1 kV/mm are imposed. It is interesting to note that this is also near the level reported by food research organisations for killing microbes (by puncture) so there may even be an increased advantage here for heat transfer operations in food processing.

This paper is concerned with combining two of these methods: surface modification and electric field application. The latter makes use of the low electrical conductivity of many fluids, especially organic fluids and refrigerants, and the resulting fact that electrical power consumption is, therefore, low, involving as it does very high voltages but very low currents. The suggestion here is that the surface distortions will cause the local electric

Address reprint requests to Dr. R. S. Neve, Dept. of Mechanical Engineering and Aeronautics, City University, Northhampton Square, London EC1V 0HB, UK.

Received 14 August 1995; accepted 15 January 1996

Int. J. Heat and Fluid Flow 17: 403–409, 1996

655 Avenue of the Americas, New York, NY 10010

0142-727X/96/$15.00
PII S0142-727X(95)00016-3

field gradient to be even greater than the value characterised by the imposed voltage divided by the gap between the electrodes or, in the case of tube heat exchangers, the logarithmic equation for field intensity in a cylindrical polar coordinate system.

## Electrohydrodynamic enhancement mechanism

The improvement in heat transfer from imposing an electric potential across heat exchanger surfaces derives from the electrohydrodynamic (EHD) force per unit volume $f_e$ generated by the electric field strength $E$, in a fluid of dielectric permittivity $\epsilon_o\epsilon$, charge density $\rho_e$, mass density $\rho$, and at temperature $T$. This can be expressed as (Stratton 1941):

$$f_e = \varrho_e E - \frac{\varepsilon_0}{2} E^2 \nabla\varepsilon + \frac{\varepsilon_o}{2} \nabla\left[E^2 \left(\frac{\partial\varepsilon}{\partial\varrho}\right)_T \varrho\right] \quad (1)$$

The first term on the right-hand side of Equation 1 is the electrophoretic force resulting from the net free charge within the fluid. The second term depends on the spatial variation of $\epsilon$ and the magnitude of $E^2$. The third term comprises the dielectrophoretic and electrostrictive components, the former resulting from the mutual effects of the thermal and electrical fields, the latter caused by any inhomogeneity of the electric field. This EHD equation must be added to the usual governing equations for fluid mechanics (Navier–Stokes) and thermal effects. There will, of course, be cross-coupling, because, for example, the force due to the electric field will become the body force (other than gravity) in the Navier–Stokes equations.

In conventional nucleate boiling, vapour bubbles generated on the heating surface grow until the buoyancy force exceeds the interfacial tension, the bubbles then being convected to the liquid's free surface. With an electric stress term present, this process will be modified, because the electric field gradient will be normal to the heating plate (usually an electric conductor) and greater at that part of the bubble farthest from the heating surface. The bubble is, therefore, subject to a squashing action, causing a thinning of the liquid film between bubble and surface and a concomitant increase in heat transfer rate. A second beneficial effect is that the bubble is apt to break up into several smaller ones following a Taylor instability in the bubble's vapour-liquid interface.

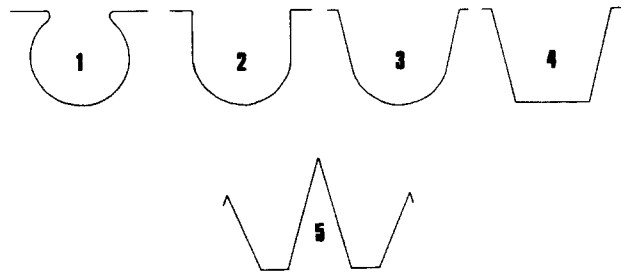


*Figure 1* Passive enhanced surface shapes used in computational analysis, (case numbers shown)

## Passive enhanced surfaces

The enhancement of heat transfer by corrugations relies on the double effect of increased surface area (compared to plan view area) and the marked difference in contact angles between bubbles and surface, the contact angle $\beta$ being defined by $\cos\beta = (\sigma_{sl} - \sigma_{vs})/\sigma_{lv}$. Five geometries are dealt with in this paper, the cross sections being as shown in Figure 1. These show a gradual metamorphosis from the shouldered cavities associated with Gewa-t$^{TM}$ surfaces (similar to Case 1) to the unequal ridge–trough alternations of Thermoexcel-C$^{TM}$ (similar to Case 5), the conventional "low fin" shape having been passed through at Case 4. Thermoexcel-HE$^{TM}$ has a much more complicated surface shape, which cannot easily be represented in pictorial form here.

It is suggested here that the advantages described in the previous section, known to result from applying an electric field to a heating surface, would be enhanced still further using these corrugated surfaces, because the electric field gradient close to corners and shoulders will be steeper than the far-field value.

## Notation

| | |
|---|---|
| $c_p$ | specific heat at constant pressure |
| $C$ | constant |
| $E$ | electric field strength (= grad $\phi$) |
| $f_e$ | electric body force per unit mass |
| $g$ | specific Gibbs function |
| $h$ | overall heat transfer coefficient |
| $H$ | latent heat |
| $J$ | nucleation rate |
| $L$ | tube length |
| $m$ | mass flow rate |
| $M$ | relative molecular mass |
| $Q$ | heat transfer rate |
| $r$ | bubble radius |
| $\Delta r$ | radial distance from electrode to mean fin radius |
| $R$ | gas constant |
| $T$ | temperature |
| $\Delta w$ | additional energy |

*Greek*

| | |
|---|---|
| $\beta$ | contact angle |
| $\epsilon$ | dielectric constant |
| $\epsilon_o$ | dielectric permitivity *in vacuo* |
| $\rho$ | mass density |
| $\rho_c$ | charge density |
| $\sigma$ | surface tension |
| $\phi$ | electric potential |

*Subscripts*

| | |
|---|---|
| *cr* | critical condition |
| *i* | inlet condition |
| lv | liquid–vapour interface |
| *o* | outlet condition |
| *s* | saturation |
| sl | surface–liquid interface |
| vs | vapour–surface interface |
| 1 | liquid phase |
| 2 | vapour phase |

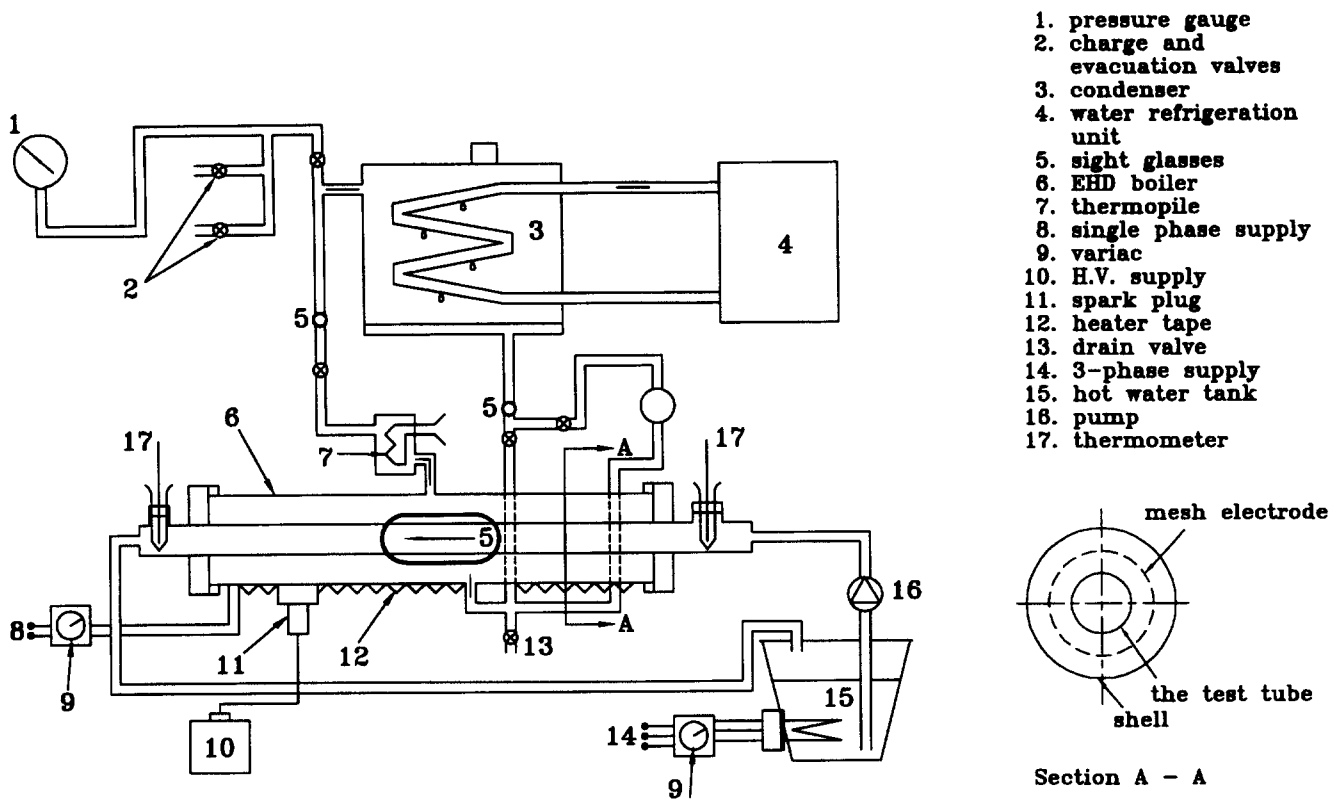


*Figure 2* Single-tube heat exchanger test rig

## Electrohydrodynamic effect on nucleation

For its equilibrium condition, the critical radius of a bubble nucleus (defined as the radius beyond which the bubble has a chance of growing in size) can be derived from the Clausius–Clapeyron equation as

$$r_{cr}^{o} = \frac{2\sigma^{o} T_s}{H \Delta T \rho_2}$$

where $\sigma^o$ is the surface tension at the vapour–liquid boundary (other variables are shown in the Notation section). From Frenkel's fluctuational theory, the kinetic nucleation rate can be written as follows:

$$J_o = C \exp\left[ -\frac{M}{R\rho_2 T}\left( \Delta g^{o} + \frac{4\pi}{3}(r_{cr}^{o})^2 \sigma^{o} \right) \right]$$

However, when the system is in the presence of an electric field and the refrigerant is a nonpolar dielectric liquid, additional energy must have been added to the system so the Gibbs free energy becomes

$$\Delta g = \Delta g^{o} + \Delta w_{1-2} = \Delta g^{o} + \left( \frac{\epsilon_o}{2} \right)(\epsilon_2 - \epsilon_1) E^2$$

and the critical radius of a generated bubble nucleus becomes

$$r_{cr} = \frac{2\sigma}{-\Delta g} = \frac{4 T_s \sigma}{2 H \Delta T \rho_2 + \epsilon_o T_s (\epsilon_1 - \epsilon_2) E^2}$$

where $\sigma$ depends closely on the external field strength. If this is uniform, $\sigma$ can be expressed as follows:

$$\sigma = \sigma^{o} - \frac{\Delta r \epsilon_o \epsilon_1}{4\pi} E^2$$

The critical radius of the nucleus, therefore, becomes the following:

$$r_{cr} = \frac{4\sigma^{o} T_s - \frac{T_s}{\pi} \Delta r \epsilon_o \epsilon_1 E^2}{2 H \Delta T \rho_2 + \epsilon_o T_s (\epsilon_1 - \epsilon_2) E^2} \tag{2}$$

and the following nucleation rate

$$J = C \exp\left\{ -\frac{M}{R\rho_2 T}\left[ \Delta g^{o} - \frac{\gamma E^2}{2} + \frac{A}{\left( 2 H \Delta T \rho_2 + \gamma T_s E^2 \right)^2} \right] \right\} \tag{3}$$

**Table 1** Tube dimensions

| Tube type | D, mm | L, mm | Wall thickness, mm | Fin pitch, mm |
|---|---|---|---|---|
| Thermoexcel-HE | 19.0 | 506 | 1.1 | 0.5 * |
| Thermoexcel-C | 19.05 | 506 | 1.24 | 0.7 |
| Gewa-T | 19.0 | 506 | 0.8 | 1.35 |
| Low fin | 19.1 | 506 | 1.2 | 0.88 |
| Smooth | 19.1 | 506 | 1.2 | N/A |

* Approximate value (difficult to quantify)

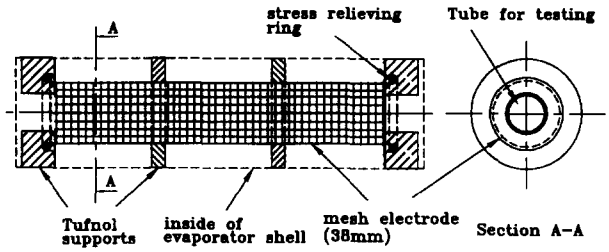


*Figure 3* Test rig mesh electrode assemblies

where $\gamma = \epsilon_o(\epsilon_1 - \epsilon_2)$, and $A = (T_s^2/3\pi^2)(4\pi\sigma^0 - \Delta r\epsilon_0\epsilon_1 E^2)^3$. The form of Equation 2 indicates that critical bubble radius will decrease with increasing electric field strength and Equation 3 indicates that nucleation rate will increase, both leading to increased heat transfer rate. A heat exchanger test rig was, therefore, assembled, modified to allow voltages up to 30 kV to be applied across the plates.

## Experimental arrangements

Figure 2 is a diagram of the single-tube test rig used in these experiments, conducted in the Thermodynamics Laboratory of the Thermo-Fluids Engineering Research Centre at City University, London. Refrigerant R114 was used as working fluid and applied voltages ranged up to 30 kV. This is now a banned fluid, used so that direct comparison could be made with previous work, but the method should apply with any refrigerant or organic fluid; that is, any nonpolar dielectric that would polarise in an electric field. The shell consisted of a brass tube 500-mm long and of 63.5-mm internal diameter. A cylindrical copper mesh electrode 38-mm in diameter was aligned coaxially with the tube, and a sight glass was positioned in the centre of the shell. The tubes were fitted with copper–constantan thermocouples for surface temperature measurement, the leads being isolated from the intense electric field by taking them out of the apparatus through the water side of the tube. Table 1 gives the dimensions of the tubes tested and Figure 3 shows the mesh electrode assemblies.

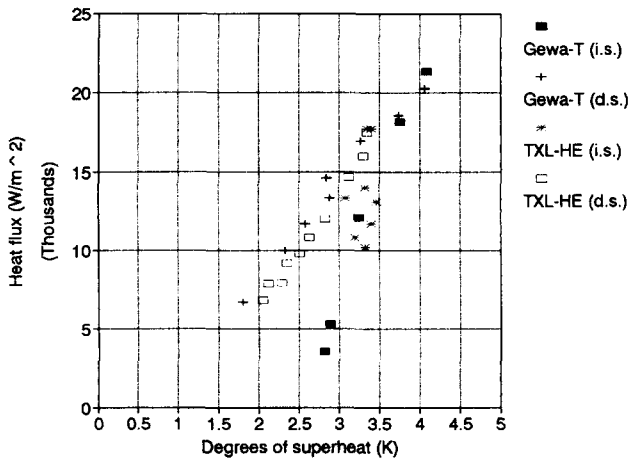


*Figure 4* Comparison of Gewa-T$^{TM}$ and Thermoexcel-HE$^{TM}$ surfaces; no applied voltage: (i.s. = increasing superheat; d.s. = decreasing superheat)

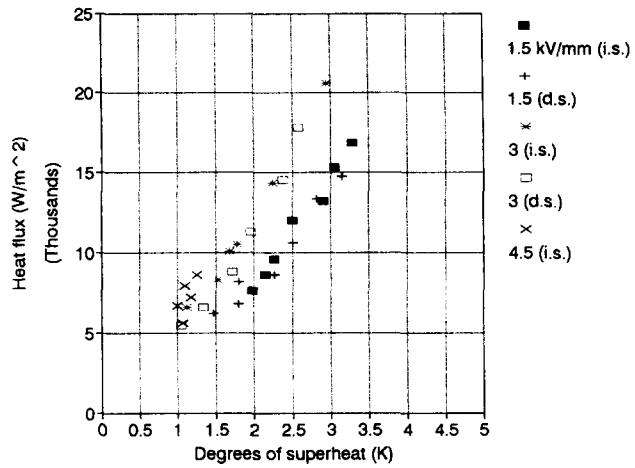


*Figure 5* Performance of Thermoexcel-HE$^{TM}$ with applied voltage

## Field strength analysis

In parallel with the experimental testing, a computational analysis was undertaken of likely electric field distributions associated with each of the surface shapes shown in Figure 1. For each case, a 1440-cell grid was set up with specified voltage boundary conditions, and Laplace's equation was then solved for potential using the PHOENICS package, marketed by CHAM Ltd. of Wimbledon, UK.

## Results

### *Experimental heat transfer tests*

In the first series of tests, Gewa-T$^{TM}$ and Thermoexcel-HE$^{TM}$ surfaces were assessed with and without an applied electric field. Figure 4 shows that with no field applied, there is a pronounced boiling hysteresis effect evident between increasing (i.s.) and decreasing superheat (d.s.) cases, especially when the degree of superheat is lower than about 3.5 K. By contrast, when an electric field strength of 1.5 kV/mm is applied to the HE surface (Figure 5), the hysteresis effectively disappears, and the heat transfer increases for the same $\Delta T$ values. The heat flux im-

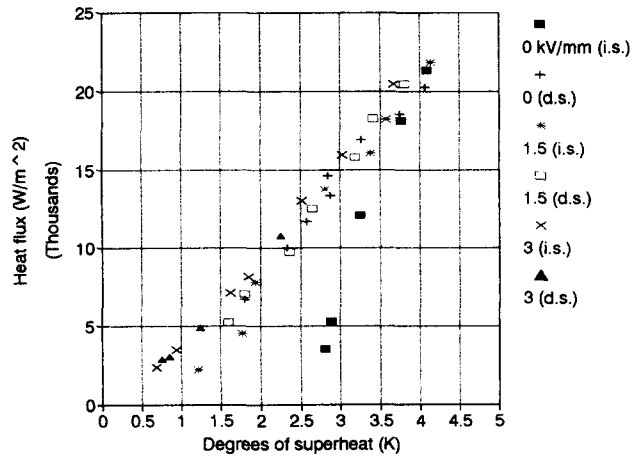


*Figure 6* Performance of Gewa-T$^{TM}$ with applied voltage

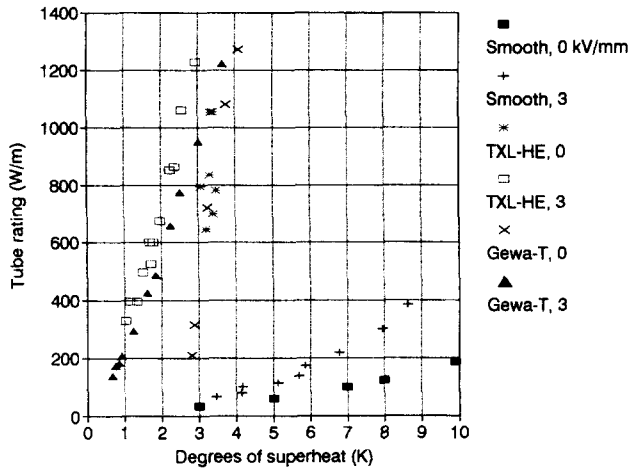


*Figure 7* Comparison of Gewa-T™, Thermoexcel-HE™, and smooth tubes, at zero and 3 kV/mm

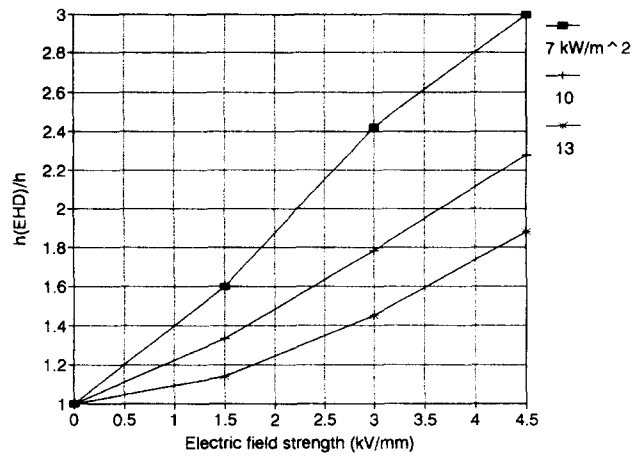


*Figure 9* Effect of applied voltage on Thermoexcel-HE™ at constant heat transfer rate

proves with double the field strength, and an extension to 4.5 kV/mm suggests that the improvements will potentially improve still further with increased voltage. In Figure 6, a similar trend is seen with Gewa-T™, hysteresis seemingly having been eliminated, within the experimental results scatter.

Figure 7 shows not only the interesting comparison of how much improvement passive enhanced surfaces give over smooth ones but also how even the smooth case is improved by a factor of about two when a 3-kV/mm electric field is applied. In this figure and the following one, the tube rating is used for comparison, defined by

$$r_m = \frac{Q}{L} = \frac{mc_p(T_i - T_o)}{L}$$

This is essential when comparing smooth tubes with passive enhanced ones, because the latter do not always lend themselves to the easy calculation of a realistic surface area. The enormous improvement in heat transfer rate at low superheat levels, using enhanced surfaces and a high voltage compared to a smooth surface, is very evident from this figure, with Thermoexcel-HE™ seeming to be the better of the two.

Figure 8 shows a comparison of two types of Thermoexcel™ surface: *HE* and *C*. For zero voltage, *HE* seems to give a better performance than *C*, but the experimental points scatter in the latter case is extreme. This superiority is retained at an applied field strength of 3 kV/mm, but beyond about 4 kV/mm, the *C* case gives a higher tube rating than *HE*, at the same $\Delta T$.

Figures 9 (for *HE*) and 10 (for Gewa-T™) show the enhancement effect of EHD voltage in terms of overall heat transfer coefficient divided by the zero-voltage value and keeping the heat transfer rate constant. Clearly, the enhancement improves with applied voltage but decreases with heat transfer rate. Nucleate boiling seems, therefore, to be controllable under these conditions.

### Field strength

Solution of Laplace's equation for the electric field strength for all of the surface geometries shown in Figure 1 using the PHOENICS package gave equipotential contours of voltage from which the field gradient could be measured to assess areas where the local value exceeded the far-field value by marked amounts. We would expect this to occur close to shoulders and points, and Figure 11 confirms this. The numbers associated with each contour in the individual cases in Figure 11 are the percentage of the full voltage applied to the opposite plate. The field distortion and bunching of contours close to corners and shoulders is quite clear.

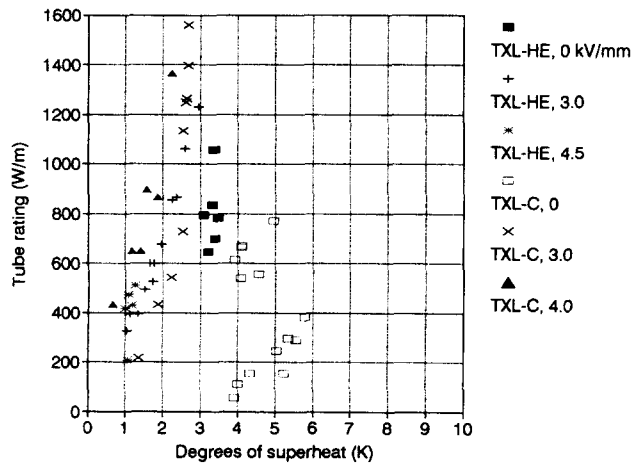


*Figure 8* Comparison of Thermoexcel-HE™ and Thermoexcel-C™

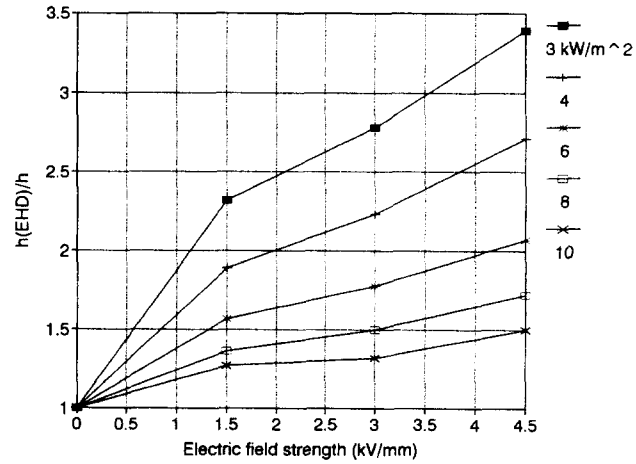


*Figure 10* Effect of applied voltage on Gewa-T™, at constant heat transfer rate

Figure 12 shows a magnified version of the contours close to the shoulders in Case 1. Although the contour smoothness has suffered slightly because of magnification, such plots enable the measurement of localised field gradients relative to the far-field value, given by the usual logarithmic relationship for cylindrical polar coordinates. In Case 1, the gradient close to the shoulders is at least three times the far-field value but, not surprisingly, the greatest localised increase in field gradient was found to be at the peaks in Case 5, where values at least 6.6 times the far-field value were indicated. This latter figure should perhaps be regarded as optimistic, because the sharpness of surface points would be difficult to maintain in industrial use. However, Case 5 closely resembles Thermoexcel-C$^{TM}$, and there is no doubt that the very impressive performance of this surface under applied voltage, as shown in Figure 8.

## Conclusions

This work has shown that valuable improvements in heat exchanger performance are to be gained from applying an electric field across the surfaces. Even with smooth tubes, a doubling of heat transfer coefficient at constant heat flux is obtained at a field strength of about 2 kV/mm, but with passive enhanced ones, there seems to be a compound effect where the improvements are proportionately even greater. This almost certainly springs from the contour distortion (and hence greater field gradient) close to shoulders and points on the surfaces, as can be demonstrated by computational solution of the field equations using a suitable finite volume or finite element technique.

Boiling hysteresis seems to be eliminated at field gradients of

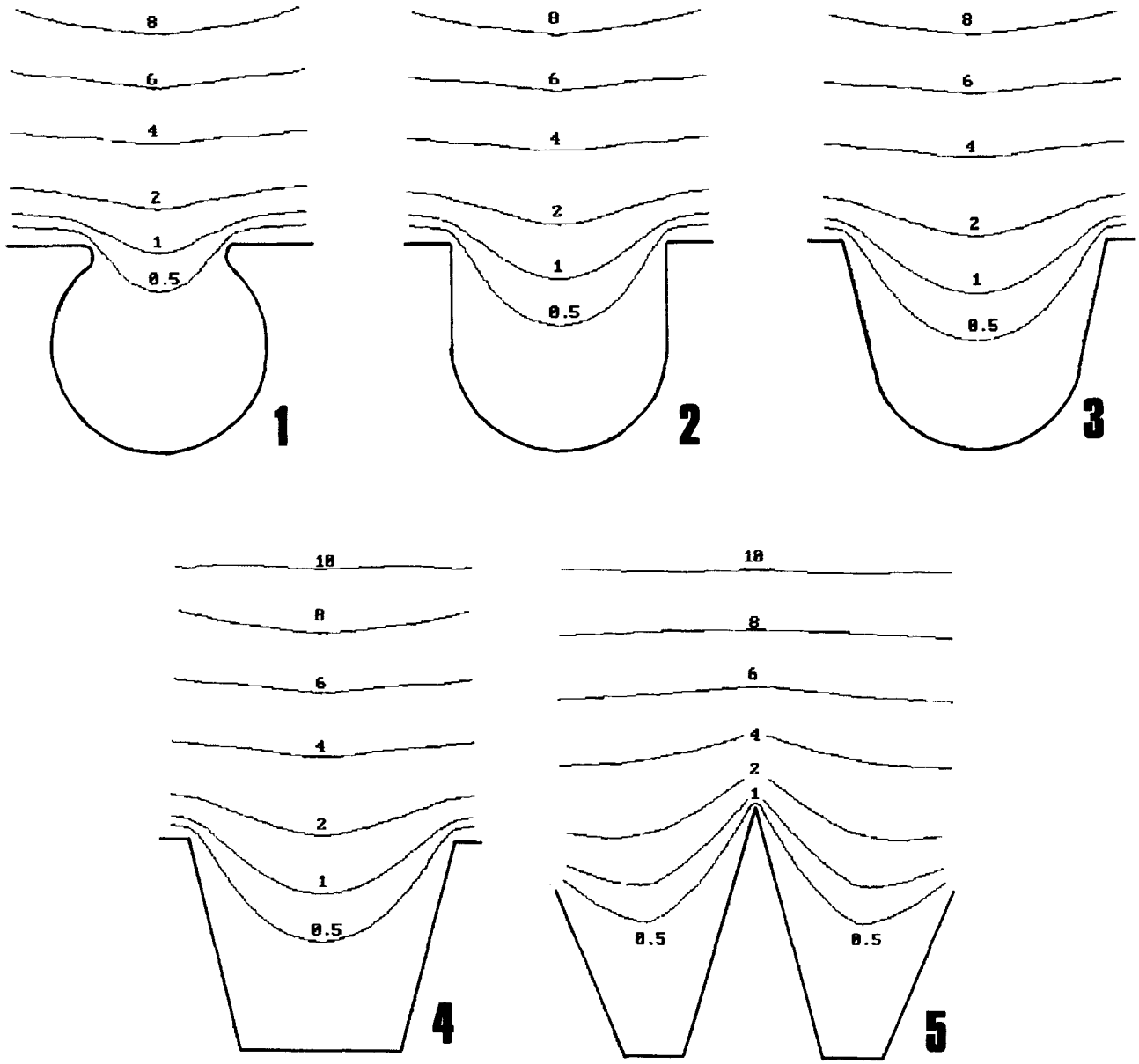


*Figure 11* Computational analysis – voltage contours for Cases 1 to 5 (numbers shown are percentages of full applied voltage)

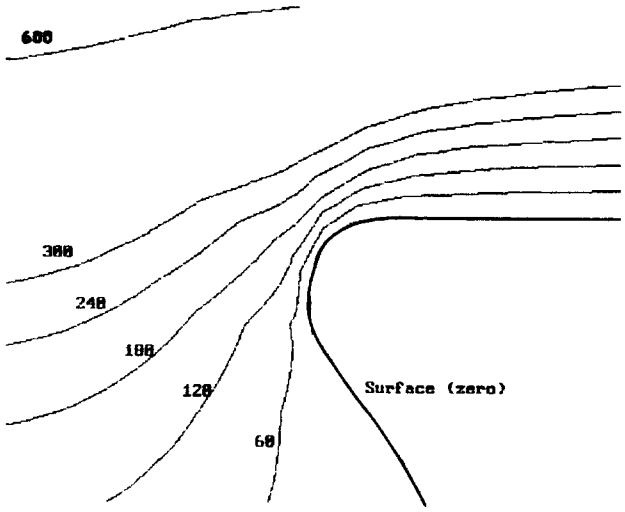


*Figure 12* Magnified view of Case 1 contours (numbers shown are in volts, for 30 kV applied)

about 1 kV/mm and further work in this area should lead to the development of an ideal surface shape for optimum performance.

## Acknowledgments

In this research project, the authors have benefitted greatly from discussions with P. H. G. Allen of City University and T. G. Karayiannis of South Bank University, London. Their help and encouragement is greatly appreciated.

## References

Allen, P. H. G. and Cooper, P. 1987. The potential of electrically enhanced evaporators. *3rd Int. Symposium on the Large-Scale Applications of Heat Pumps*, Oxford, UK, 221–229

Barletta, A. and Zanchini, E. 1993. On the stress tensor for a dielectric fluid in an electrostatic field. *Int. J. Heat Technol.*, **11**, 159–176

Bergles, A. E. 1985. Techniques to augment heat transfer. In *Handbook of Heat Transfer Applications*, 2nd ed., W. M. Rohsenow, J. P. Hartnett, and E. N. Ganic (eds.), McGraw-Hill, New York

Bergles, A. E. 1989. The challenge of enhanced heat transfer with phase change. *Proc. 7th National Heat Transfer Conference*, Firenze, Italy, 1–12

Choi, H. 1961. Electrohydrodynamic boiling heat transfer. Mechanical Engineering Dept. Report 61-12-1, Tufts University, Medford, MA, USA

Choi, H. 1962. Electrohydrodynamic boiling heat transfer. Ph.D. Thesis, Mechanical Engineering Dept., MIT, Cambridge, MA, USA

Cooper, P. 1990. EHD enhancement of nucleate boiling. *ASME, J. Heat Transfer*, **112**, 458–464

Jones, T. B. 1978. Electrohydrodynamically enhanced heat transfer in liquids — A review. In *Advances in Heat Transfer*, Vol. 14, Academic Press, New York, 107–148

Karayiannis, T. G., Collins, M. W. and Allen, P. H. G., 1989. Electrohydrodynamic enhancement of nucleate boiling heat transfer in heat exchangers. *Chem. Eng. Comms.*, **81**, 15–24

Ogata, J. and Yabe, A. 1993. Basic study on the enhancement of nucleate boiling heat transfer by applying electric fields. *Int. J. Heat Mass Transfer*, **36**, 775–782

Ohadi, M. M., Paper, R. A., Ng, T. L., Faani, M. A. and Radermacher, R. 1992. EHD enhancement of shell-side boiling heat transfer coefficients of an R-123/oil mixture. *Trans. ASHRAE*, **92**

Stratton, J. A. 1941. *Electromagnetic Theory*. McGraw-Hill, New York

Webb, R. L. and Pais, C. 1992. Nucleate pool boiling data for five refrigerants on plain, integral-fin, and enhanced tube geometries. *Int. J. Heat Transfer*, **15**, 1893–1904